Procedure for Automated Virtual Optimization of Variable Blank Holder Force Distributions for Deep-Drawing Processes with LS-Dyna and optiSLang

Klaus M. Wurster[1,2*], Mathias Liewald[1,2], Christian Blaich[2], Matthias Mihm[2]

[1] GSaME – Graduate School of Excellence advanced Manufacturing Engineering, Stuttgart

[2] Institute for Metal Forming Technology, University of Stuttgart

Abstract

Components for passenger car bodies represent one of the largest fields of application of sheet metal forming processes. Distinctive passenger car design in combination with constantly increasing lightweight requirements led to new challenges for deep-drawing processes. Hence, new strategies to enlarge process windows of manufacturing processes as such were necessary. One possibility to manage quality of deep drawn components is given by variation of blank holder force during forming process. The present article describes a procedure for automated optimization of blank holder force distribution for a deep-drawing process with segment-elastic blank holder. Thereby, it was possible to identify optimized blank holder force distribution in space and time without manual investigation of optimization results during finite element analysis prior to manufacturing of deep-drawing die.

Keywords: optimization, deep-drawing, variable blank holder force distribution

[*] Contact: Dipl.-Ing. Klaus M. Wurster, Graduate School of Excellence advanced Manufacturing Engineering, Nobelstrasse 12, 70569 Stuttgart, mailto: klaus.wurster [@] gsame.uni-stuttgart.de

1 Introduction

With regard to volatile developments of market segments from a sellers to a buyers market behaviour, distinctive passenger car design has become one of the major selling points in automotive industry. At the same time, regulation of CO_2 emissions increased lightweight design requirements in passenger car body production. In comparison to steel, formability of lightweight materials, such as aluminium, looks more challenging. To obtain robust processes, it is therefore necessary to develop strategies to enlarge process windows and to optimize utilization of entire operational range. To reduce time-to-market, virtual methods for evaluation of deep-drawing processes, such as finite element analysis (FEA), gain in importance today. In this context, automated methods for evaluation of failure criteria, such as wrinkling and cracks, are important for a time-saving and cost-effective determination of optimized input parameters for robust deep-drawing processes. The present article describes a method to optimize blank holder force distribution of a deep-drawing process in space and time. Hereby, LS-Dyna, optiSLang, LS-PrePost and Microsoft Excel were combined to obtain an automated procedure.

2 Control of Material Flow in Deep-Drawing Processes

In production of passenger car body components, deep-drawing is one of the most important manufacturing processes (Lange, 1990). A usual deep-drawing die is shown in figure 1. It consists of a die cavity, a blank holder and a punch.

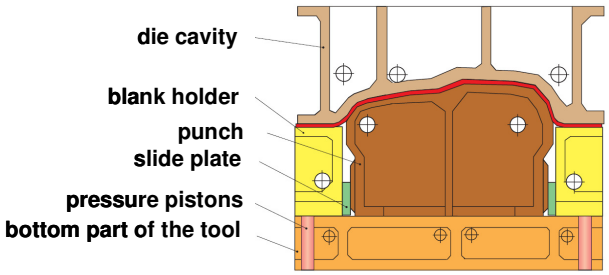

Figure 1: Deep-drawing die (Schuler, 1996)

During the deep-drawing process, the blank is clamped between die cavity and blank holder. The blank holder is to avoid the occurrence of wrinkling and inducing required retracking force. While the punch is forming the blank into the die cavity, blank material flows into die cavity. This effect is called material flow. In deep-drawing processes, it is important to control material flow in order to get defect-free components. Main defects in deep-drawing processes are cracks and sidewall wrinkling, depicted in figure 2 (Beck, 2004).

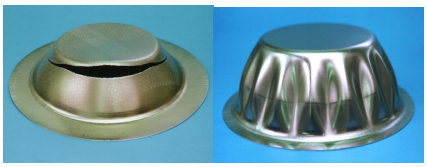

Figure 2: Cracks and sidewall wrinkling in a conical cup (Beck, 2004)

Material thinning and cracks may arise when local load in the blank increased the level of uniform elongation. In contrast, sidewall wrinkling occurred when tangential compressive stresses led to buckling in the sidewall area (Lange, 1990).

In deep-drawing, wrinkling and cracks have to be avoided by control of material flow. Blank holder force, draw or lock beads, type and amount of lubricant as well as shape and size of initial blank represent possibilities to influence material flow. (Zuenkler, 1985; Sommer, 1987; Siegert, 1991) The present work focused on material flow control utilizing different amount and variable distributions of blank holder force. One of the variable blank holder forces known from literature has been published by Sheng (Sheng 2003) and is illustrated in figure 3. The depicted blank holder force profile has been utilized for optimization of deep-drawing a conical cup.

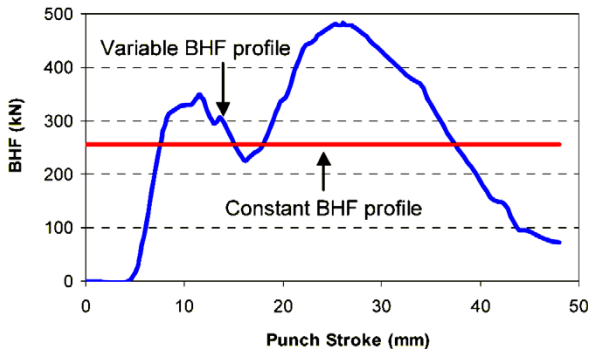

Figure 3: Variable blank holder force for a conical cup (Sheng, 2003)

The variable blank holder force reached a local maximum at a draw depth of about 10 mm. After decreasing below the level of the referring constant blank holder force, the global maximum was reached at a draw depth of about 27 mm. Afterwards blank holder force decreased constantly.

Within the present article, optimization of variable blank holder force distributions was tested for a fender shaped geometry described hereinafter.

3 Fender Shaped Geometry and Deep-Drawing Die

Deep-drawing processes often are used to produce passenger car body components. For that reason, one component geometry similar to a front fender of a passenger car has been chosen for the investigations.

Within finite element analysis (FEA) investigated fender shaped geometry and referring die are shown in figure 4. The sheet metal component has a length of 642 mm and a width of 415 mm. The component has four different corner radii and due to the tapered walls with four different angles, the presented geometry tends to fail by sidewall wrinkling (Haeussermann, 2002).

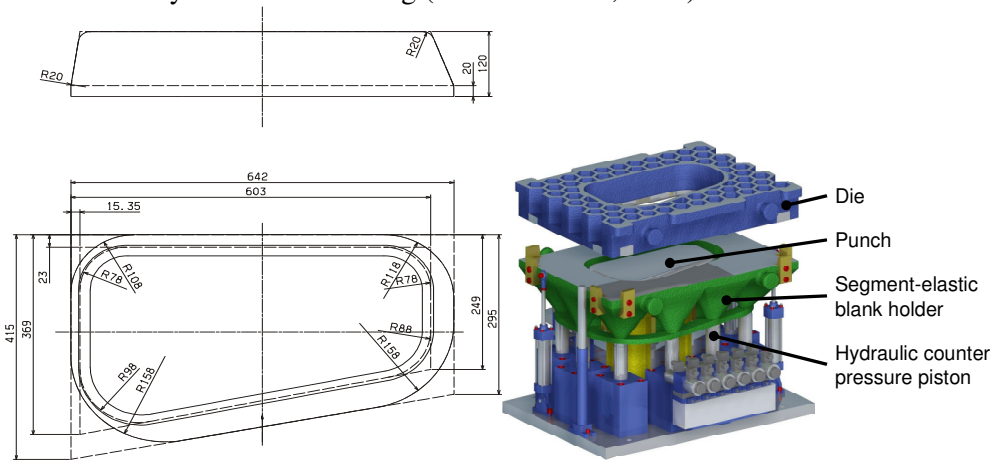

Figure 4: Dimensions of punch and deep-drawing die set with segment-elastic blank holder (Haeussermann, 2002)

The die set depicted in figure 4 has been developed at IFU. (Haeussermann, 2002) It contains a segment-elastic blank holder that consists of ten blank holder segments. Each segment has a separate hydraulic pressure piston to transfer specific local pressure into the blank holder segment. The design of the blank holder segments as truncated pyramids ensures uniform distribution of the pressure within the blank holder segment. A cover plate connects the individual blank holder segments. It avoids marks on the sheet metal component resulting from the separating line between the individual blank holder segments. The FE-model of the fender shaped geometry is described in the following.

4 FE-Model of Fender Shaped Geometry

Prior to manufacturing of deep-drawing die sets, analysis of the referring processes is accomplished by finite element analysis (FEA). The presented FE-model has been developed for utilization in LS-Dyna (Liewald, 2009). Blank holder, die and punch were modelled as rigid bodies in order to reduce computation time. Depending on rolling direction, sheet metal shows different material properties. Utilization of 3-parameter Barlat material model (type 36) enables implementation of Lankford parameters r_0, r_{45} and r_{90} into the FE-model. Thus, it was possible to include variety of material properties dependent on rolling direction in FE-model. The FE-model of the sheet material virtually has been divided into eleven component areas. Thus, result evaluation in every single component area adjacent to referring blank holder segment was enabled. The FE-models of the blank holder segments and of the sheet metal component are shown in figure 5.

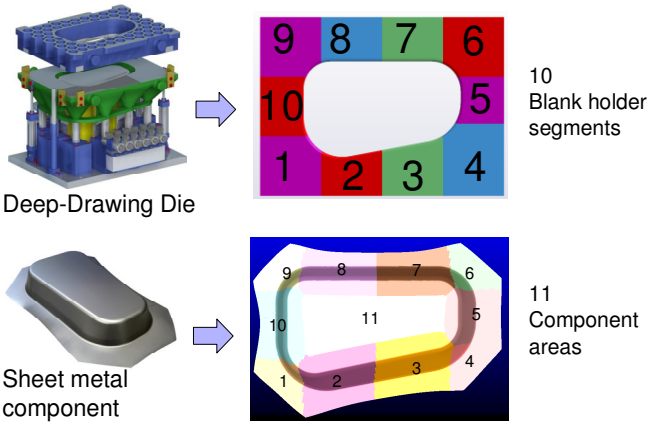

Figure 5: Deep-drawing die and FE-model of segment-elastic blank holder (top), sheet metal component with FE-model of eleven component areas (bottom) (Blaich, 2010)

5 Automated Failure Detection in FEA

One can detect failure criteria sidewall wrinkling and cracks in FEA. However, occurrence of sidewall wrinkling often was evaluated manually. To enable a time-efficient evaluation of FEA results, an automated method to evaluate occurrence of sidewall wrinkling has been developed and is described in the following.

5.1 Sidewall Wrinkling Criteria

Deep-Drawing components mostly fail by crack or sidewall wrinkling. In literature, different approaches for detection of sidewall wrinkling have been found. Dependent on their functionality, they are divided into stress based, energy based, geometry based and formability based methods. The guideline VDI 3417 describes a method to identify sidewall wrinkling based on second principle stress. Cao (Cao, 2000) pointed out an energy based method for detection of sidewall wrinkling. Hence, sidewall wrinkling occurred when mechanical work transferred by modified shell element forces exceeds level of critical energy required for formation of wrinkling. Another method to detect sidewall wrinkling is the comparison of the sheet metal component with a geometrically perfect component. If deviation exceeds the limit of 20 percent of initial blank thickness, sidewall wrinkling occurs (Sheng, 2004; Zhang, 2008). Doege and Kracke (Doege, 1998) identified the occurrence of sidewall wrinkling utilizing strain distribution in forming limit diagram. Based on experiments, wrinkling limit curves for forming limit diagram have been identified. Evaluation and testing of different sidewall wrinkling criteria for FEA determined most suitable wrinkling criterion. According to these investigations, wrinkling criterion based on strain ratios φ_1 / φ_2 in forming limit diagram was implemented in FEA. In a first step, this wrinkling criterion has been evaluated for a conical cup. Sidewall wrinkling was initiated in the area at one third of final draw depth (Simon, 1996). For this reason, evaluation

of elements within this area was appropriate to identify sidewall wrinkling and reduce computation time. The wrinkling limit curve consisted of a straight line through the origin. By use of mild steel DC04 with an original blank thickness of 0.9 mm the gradient of the curve was -1.22 for the conical cup and -1.55 for fender shaped geometry (Blaich, 2010). When φ_1 / φ_2 ratios within this area content values below the wrinkling limit curve, sidewall wrinkling occurred. An example is shown in figure 6.

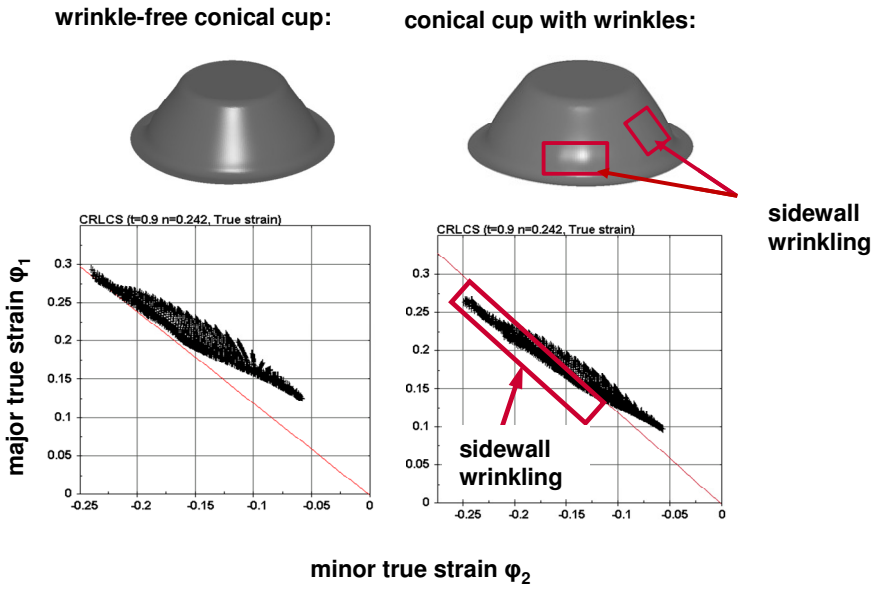

Figure 6: Wrinkling limit cure in forming limit diagram for a conical cup (Liewald, 2010)

After successful testing of conical cup, most suitable wrinkling criterion was transferred to fender shaped geometry described in chapter 3. The tests have shown that described sidewall wrinkling criterion is suitable for automated detection of sidewall wrinkling for conical cup and fender shaped geometry. In combination with automated evaluation of maximum thinning, implementation of a procedure to optimize process input parameters with regard to failure criteria cracks and sidewall wrinkling at the same time was possible.

5.2 Automated Detection of Sidewall Wrinkling in FEA

Design requirements and time efficiency have a lasting effect on development processes. To meet these requirements, automated sidewall wrinkling detection in FEA of deep-drawing processes is a necessity. Gradient of wrinkling limit curve and φ_1 / φ_2 ratios represent measurable dimensions. They enable consistent evaluation of occurrence of sidewall wrinkling. Implementation of such wrinkling criterion in widely known optimization software optiSLang avoided time consuming manual investigation of simulation results. Combination of automated detection of sidewall wrinkling with limit value indicating maximum thinning

allowed optimization of blank holder force to produce defect-free passenger car components. The developed method utilized optiSLang, LS-Dyna, LS-PrePost and Microsoft Excel. The batch procedure is depicted in figure 7 (Liewald, 2011).

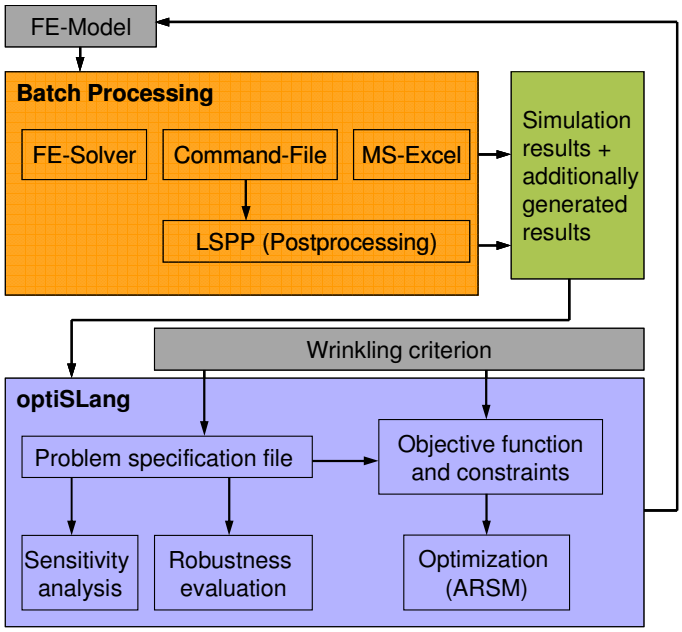

Figure 7: Procedure for automated sidewall wrinkling detection in FEA (Liewald, 2011)

The batch processing software controlled FE-solver, LS-PrePost and Microsoft Excel. First, FE-model was transferred to FE-solver. Then, FE-calculations were started. Following the calculations, LS-Prepost was started to determine material thinning in the entire component and pairs of variates of strain distribution in forming limit diagram for the chosen band of elements. A command file controlled the command sequences in LS-PrePost. By opening Microsoft Excel in a next step within batch processing, Visual Basic for Application (VBA) programs in Excel were started automatically. These macros imported results of strain distribution, calculated φ_1 / φ_2 ratios and sorted them into descending order. Evaluation of φ_1 / φ_2 ratio as well as determination of material thinning was done separately for every single component area. Thereby, local effects on thinning and occurrence of sidewall wrinkling have been analysed. The developed procedure is implemented into optimization procedure to find most suitable blank holder force distribution as follows.

6 Virtual Automated Optimization of Blank Holder Force Distribution in FEA of Deep-Drawing Processes

In this section, implementation of variable blank holder force distributions into dedicated FEA procedure is shown. Afterwards, optimization results are described.

6.1 Integration of Variable Blank Holder Force Distributions in FEA of Deep-Drawing Processes

The present article describes possibilities to implement variable blank holder force distributions into FEA through the example of the FE-solver LS-Dyna. In dynamic explicit FEA, it is possible to divide the simulation time into ten time steps. A specific amount of blank holder force is assigned to every single time step. Thus, variable blank holder force distributions were approximated trough a set of ten support points. With regard to possible blank holder force settings of the sheet metal forming press, upper and lower boundaries of the single blank holder force were chosen. Therefore, this method was called tolerance margin method. One of the advantages of the tolerance margin method was the easy implementation in FEA. In a die set with a segment-elastic blank holder consisting of ten individual blank holder segments, ten support points in every single blank holder segment result in 100 optimization parameters necessary for optimization of variable blank holder force distribution. This resulted into development of a method that enables reduction of number of optimization parameters. One solution to achieve this goal was the implementation of a variable blank holder force distribution as a mathematical function directly in preprocessing of FEA. In this case, number of parameters to describe variable blank holder force distribution is reduced depending on degree of underlying mathematical function.

Within sensitivity analysis with optiSLang, it has been shown, that individual blank holder segments show different significance on the occurrence of cracks and sidewall wrinkling (Blaich, 2010). Therefore, another approach to reduce quantity of optimization parameters is given by results of sensitivity analysis. Thus, tolerance margin method was applied to significant segments only. The procedure for optimization of variable blank holder force distribution in deep-drawing of a fender shaped geometry is described in the following.

6.2 Procedure for Automated Virtual Optimization of Variable Blank Holder Force Distribution

For automated virtual optimization of variable blank holder force distribution for deep-drawing of fender shaped geometry, the procedure described in table 1 has been chosen.

Table 1: Procedure for optimization

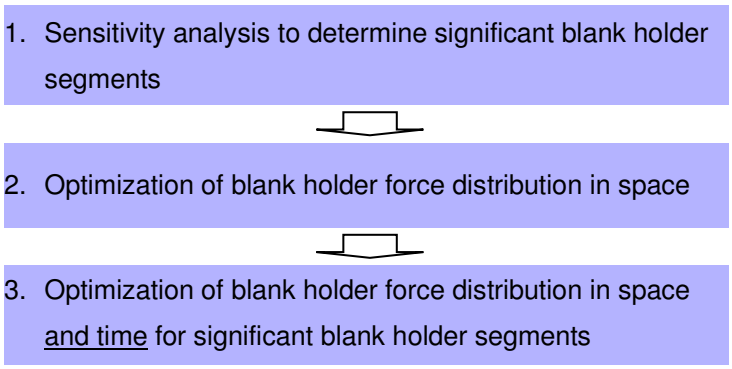

In a first step, sensitivity analysis was carried out. Thereby, blank holder segments significant to failure by cracks and sidewall wrinkling were determined. Afterwards, blank holder force distribution of segment-elastic blank holder variable in space was optimized. This means, that the amount of blank holder force were different in the individual blank holder segments but individual blank holder forces were constant during deep-drawing process. Optimization of blank holder force distribution was completed by a final optimization of blank holder force distribution variable in space and time. In addition to locally different amounts of blank holder forces, the meaning of variable in space and time also included variation of blank holder force during deep-drawing process. This last optimization step was accomplished utilizing tolerance margin method for significant blank holder segments only. The automated procedure for result evaluation was used in every optimization step and led to the results described in the following.

7 Optimization Results

This section gives an overview of the optimization results achieved in FEA. First of all, results of sensitivity analysis are described. Afterwards, results of optimization of blank holder force distribution variable in space and time are shown.

7.1 Results of Sensitivity Analysis

In a first step, optiSLang was used for sensitivity analysis. Basis for the investigation was a simulation with a constant blank holder force of 140.000 N in every single segment of the segment-elastic blank holder. The simulation results are shown in figure 8.

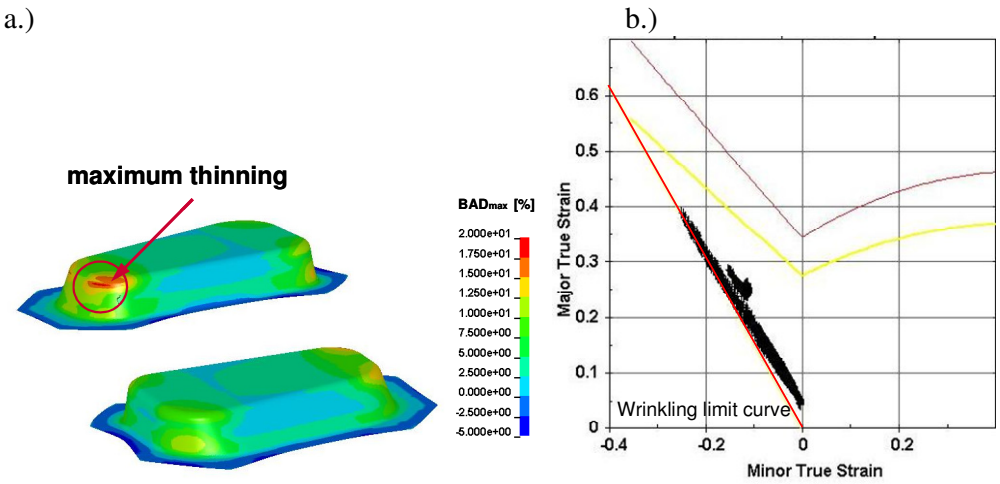

Figure 8: Initial simulation results for sensitivity analysis and optimization, thinning (a) and strain distribution (black) in forming limit diagram (b)

Maximum thinning of 18.55% arised within red marked component area This component area is adjacent to blank holder segment No 6 (figure 9). In forming limit diagram (figure 8b), strain distribution (black) locally reached the area below the wrinkling limit curve. This result confirmed occurrence of slight sidewall wrinkles also detected in visible investigation.

Within sensitivity analysis the ten blank holder forces may vary ± 50% of the initial value. Latin hypercube method has been used for generation of 70 samples to represent the parameter space. Evaluation of coefficient of importance shows that blank holder force was suitable to influence material thinning and occurrence of sidewall wrinkling. Additionally, significant blank holder segments have been identified and are depicted in figure 9 (green).

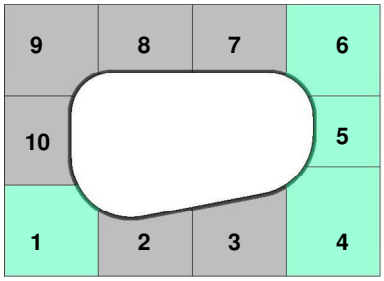

Figure 9: Segment-elastic blank holder with significant segments (green)

In a next step the ten blank holder forces have been optimized in space. Blank holder forces may be different in the individual blank holder segments but constant during deep-drawing process.

7.2 Results of Optimization of Blank Holder Force Variable in Space

This section gives an overview of the results achieved in optimization of blank holder force variable in space. The adaptive response surface method with default settings has been utilized to identify optimized combination of locally different blank holder forces. The ten blank holder forces of the segment-elastic blank holder have been optimization parameters. Minimization of thinning has been the objective function (1). Wrinkling limit curve was implemented as constraint (2).

$$\text{“Minimize } BAD_{max}\text{”} \tag{1}$$

$$0 \leq fabs(FLDG/-1.55)-1 \tag{2}$$

The optimization run converged after 14 iterations and 270 designs. The blank holder force distribution of the best design number 255 is shown in figure 10

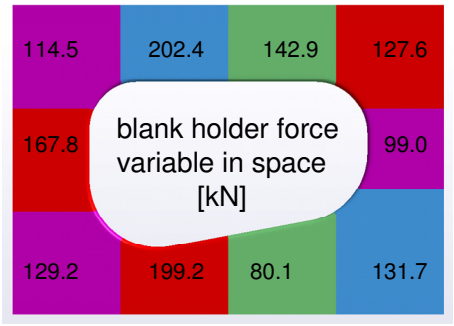

Figure 10: Blank holder force distribution variable in space

The segment forces vary between 80.1 kN in segment 3 and 202.4 kN in segment 8. This effect shows that upper (210 kN) and lower (70 kN) boundaries have been suitable for optimization purposes. Such blank holder forces resulted in the material thinning depicted in figure 11.

a.) b.)

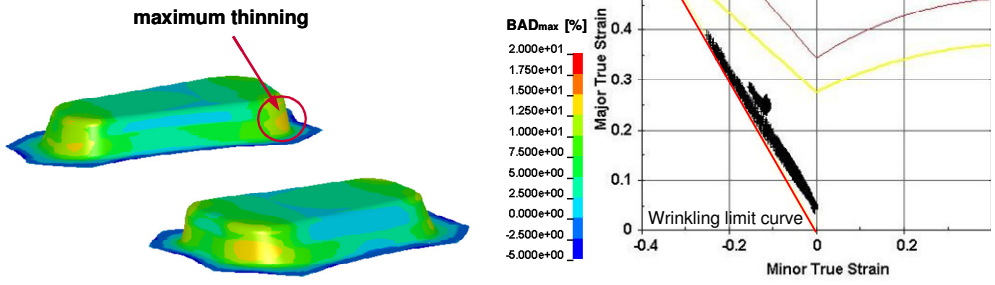

Figure 11: Optimization result of blank holder force variable in space, thinning (a) and strain distribution (black) in forming limit diagram (b)

Maximum thinning of 14.97% arised in the red circled component area (figure 11a). Hence, the component did not fail by cracking. In forming limit diagram (figure 11b), strain distribution is plotted for the band of elements (black) in the area where sidewall wrinkling starts to develop. The strain distribution has reached the area close to the wrinkling limit curve, but there are no pairs of variates below the wrinkling limit curve. Thus, no sidewall wrinkling occurs. Compared to initial simulation set up, optimization variable in space reduces maximum thinning by 19%. At the same time, the occurrence of sidewall wrinkling is avoided and hence, the component is defect-free. The automated procedure for optimization of blank holder force distribution has afterwards been utilized for implementation of variable blank holder force distributions in significant segments of sensitivity analysis. The results are described in the following.

7.3 Results of Optimization in Space and Time

Based on the results of sensitivity analysis and automated optimization of blank holder force distribution variable in space, blank holder force distribution of significant blank holder segments has been optimized variable in time utilizing objective function (1) and constraint (2). To do so, automated optimization with tolerance margin method has been utilized in the significant blank holder segments. Within this procedure blank holder force during deep-drawing process has been defined utilizing ten support points. The blank holder force of every support point was limited by the lower boundary of 70 kN and the upper boundary of 210 kN. Implementation of ten support points in four significant blank holder segments led to 40 optimization parameters. Due to the number of optimization parameters, evolutionary algorithm has been chosen for optimization. The optimization converged after 230 designs. The results of best design 218 are illustrated in figure 12.

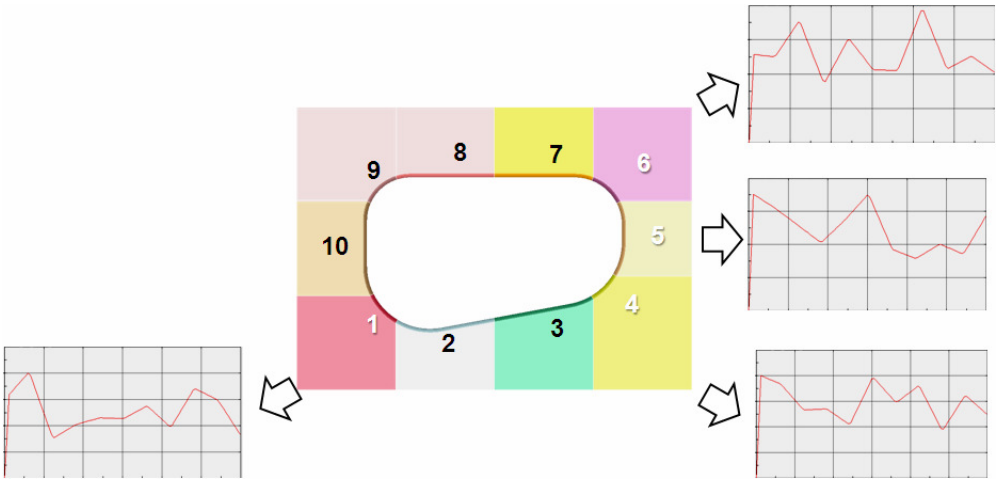

Figure 12: Blank holder force distributions variable in time

The illustrated blank holder force distributions variable in time do not exactly refer to a typical distribution known from literature. The distributions did not reach the given boundaries. Therefore, upper (210 kN) and lower (70 kN) boundaries are suitable for optimization. With respect to control possibilities during deep-drawing process, fitting curves were applied on results of variable blank holder force distributions. Implementation of fitting curves did not have a significant influence on FEA results. Combination of optimization results in space with optimization results in time led to simulation results depicted in figure 13.

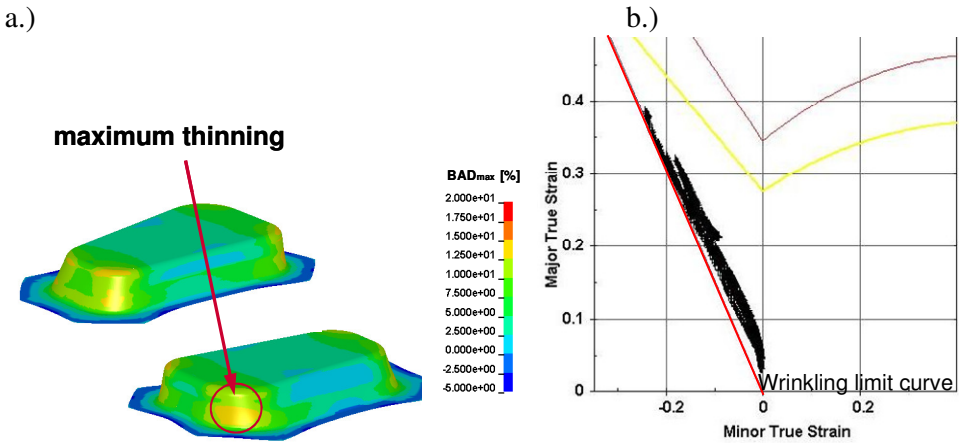

Figure 13: Optimization results of blank holder force variable in space and time, thinning (a) and strain distribution (black) in forming limit diagram (b)

Maximum thinning of 14.51% arised in the red circled component area. Hence, the component did not fail by cracking. In forming limit diagram, strain distribution has been plotted for the band of elements in the area where sidewall wrinkling started to develop. The strain distribution has reached the area close to the wrinkling limit curve, but there were no pairs of variates below the wrinkling limit curve. Thus, no sidewall wrinkling occurs. Compared to initial simulation set up, blank holder force variable in space and time reduced maximum thinning by 22%. At the same time, the occurrence of sidewall wrinkling has been avoided and hence, the component is defect-free. In comparison to optimization of blank holder force distribution variable in space, the implementation of blank holder forces variable in space and time reduced maximum thinning by 3% again.

8 Conclusions

The present article describes a procedure for automated detection of sidewall wrinkling in FEA of deep-drawing processes. This method has been applied in optimization of blank holder force to avoid failure by crack or sidewall wrinkling. The method has been tested successfully for a conical cup and afterwards it has been implemented in deep-drawing of a fender shaped geometry. In a next step, procedures for automated optimization of blank holder force distributions variable

in time have been developed and tested. The so called tolerance margin method has been utilized for further optimization runs.

Within these optimization runs, significant blank holder segments of a segment-elastic blank holder have been identified by applying particular sensitivity analysis. In a next step, blank holder force distribution variable in space has been optimized by using adaptive response surface method. The results showed a defect-free part without sidewall wrinkling and reduced maximum thinning by 19% compared to initial simulation. Afterwards, tolerance margin method was used for significant segments' optimization of blank holder force distribution variable in time. This method provided the possibility to reduce thinning by 3% again. At the same time, the defect-free part did not show any sidewall wrinkling. The developed automated procedure for optimization increased time-efficiency and eliminated diversity in interpretation of simulation results.

References

BECK, S.; *Optimierung der Zargenspannung beim Ziehen unregelmaessiger Blechformteile,* Universitaet Stuttgart, Dissertation, 2004

BLAICH, C.; LIEWALD, M.; Erfassung und Regelung lokaler Zargenspannungen zur Optimierung von Tiefziehprozessen, In: *Neuere Entwicklungen in der Blechumformung,* Herausgeber: M. Liewald, Werkstoff-Informationsgesellschaft, 2010

CAO, J.; WANG, X.; On the Prediction of side-wall wrinkling in sheet metal forming processes; In: *International Journal of Mechanical Sciences 42*, 2000

DOEGE, E.; KRACKE, M.; Vorhersage der Faltenbildung in geneigten Ziehteilzargen mit elementaren Ansaetzen, In: *Blech, Rohre und Profile 11/2998*, S. 54-61, 1998

HAEUSSERMANN, M.; *Zur Gestaltung von Tiefziehwerkzeugen,* Universitaet Stuttgart, Dissertation, 2002

LANGE, K.; *Umformtechnik – Handbuch fuer Industrie und Wissenschaft, Band 3: Blechbearbeitung*, Springer-Verlag, Berlin, Heidelberg, New York, 1990

LIEWALD, M.; BLAICH, C.; Approaches for Closed-loop Control and Optimization of Deep Drawing Processes, In: *Proceedings of the ANSYS Conference and 27th CADFEM Users' Meeting,* Leipzig, 2009

LIEWALD, M.; WURSTER, K.; BLAICH C.; Approaches for Automated Sidewall Wrinkling Detection in Deep-Drawing Processes, In: *Proceedings of the 11th Stuttgart International Symposium Automotive and Engine Technology,* Stuttgart, 2011

SCHULER, *Handbuch der Umformtechnik*, Schuler GmbH, Springer-Verlag, Berlin, London, New York, 1996

SHENG, Z.Q.; JIRATHEARANAT, S.; ALTAN T. Adaptive FEM simulation for prediction of variable blank holder force in conical cup drawing, In: *International Journal of MachineTools & Manufacture, Vol. 44,* 2003

SHENG, S.; SHIVPURI, R.; *Adaptive PI Control Strategy for Prediction of Variable Blank Holder Force,* ESAFORM Conference on Material Forming, Trondheim, 2004

SIEGERT, K.; Grundlagen der Blechumformung unter tribologischen Gesichtspunkten, In: *Lehrgang Tribologie und Schmierung in der Umformtechnik,* Technische Akademie Esslingen, 1991

SOMMER, N.; Niederhalterdruck und Gestaltung des Niederhalters beim Tiefziehen von Feinblechen, In: *Industrie-Anzeiger 109*, Heft 9, S. 32-33, 1987

ZUENKLER, B.; Zur Problematik des Blechhalterdrucks beim Tiefziehen, In: *Bleche, Rohre und Profile 32,* Heft 7, S. 323-326, 1985